Contribution from the Chemistry Department,
University of Tasmania, Hobart, Tasmania 7001, Australia

# Temperature Dependence of the Electronic Spectrum of the Planar $CuCl_4^{2-}$ Ion: Role of the Ground- and Excited-State Potential Surfaces

Mark J. Riley and Michael A. Hitchman*

*Received March 3, 1987*

The cause of the unusual temperature dependence of the previously reported d–d electronic spectrum of the planar $CuCl_4^{2-}$ ion has been investigated. The variation of the intensity of the $^2A_{1g}(z^2) \leftarrow {}^2B_{1g}(x^2-y^2)$ transition in $z$ polarization suggests that the potential surface of the ground state in the out of plane inducing coordinate of $\beta_{2u}$ symmetry is slightly anharmonic. A moments analysis has shown that the unusually large red shift which occurs in the band maximum on warming from 10 to 295 K is quite inconsistent with excited-state potential surfaces which are similar to those in the ground state. The angular overlap model of the bonding in metal complexes has been used to derive excited-state potential surfaces for each normal coordinate, and in every case except the $\alpha_{1g}$ and $\beta_{2u}$ vibrations these differ from those in the ground state merely by having somewhat reduced force constants. For the $\alpha_{1g}$ mode, as expected, a displacement occurs that corresponds to a lengthening of each Cu–Cl bond. For the $\beta_{2u}$ vibration, the calculations imply a highly flattened excited-state potential with double minima corresponding to two equivalent distorted tetrahedral ligand geometries. The band shifts calculated with these excited state surfaces are still in poor agreement with those observed experimentally. However, it is shown that an excited-state potential with double minima deeper than those estimated by using the angular overlap model produces simulated spectra that agree well with those observed experimentally, not just as far as the shifts in band maximum with temperature are concerned. They also reproduce the shift in energy between $z$ and $xy$ polarization. The basic causes of the spectral band shape of the transition are discussed, and the implications of these on the interpretation of vibronically induced electronic transitions are considered.

## Introduction

It is generally accepted that the intensity of the formally forbidden "d–d" transitions of centrosymmetric transition-metal complexes is derived by vibronic coupling with higher energy parity-allowed transitions.[1] However, although the Herzberg–Teller theory describing the process is well established,[2] this has been tested experimentally for comparatively few compounds. An important class of complexes where considerable data are available is that of the planar ions of the type $MX_4^{2-}$, where M = Pt, Pd, or Cu and X is a halide ion.[3-5] These have the advantage that the transitions between individual d orbitals may generally be resolved by using polarized light. Moreover, the normal vibrations of the complexes are simple and well characterized, which greatly aids in the interpretation of the effects of vibronic coupling.

The low-temperature spectra of the Pt(II) and Pd(II) complexes show considerable vibrational fine structure, and analysis of this has provided a detailed picture of the nature of the intensity-inducing vibrations and the changes in metal–ligand bond lengths that accompany some of the d excitations in these compounds.[3] The spectra of three compounds containing planar $CuCl_4^{2-}$ have been studied in detail to date.[4,5] While similar in general terms, these differ in the extent to which vibrational structure may be resolved at low temperature, though where observed, this was analyzed in a manner similar to the analogous tetrachloroplatinum(II) and -palladium(II) species. An additional common feature of the spectra of the copper(II) complexes is a dramatic increase in the intensity of some of the bands as the temperature rises from 10 to 295 K, and this has been analyzed quantitatively in terms of the *ungerade* vibrations that are involved in the vibronic coupling.

A particularly unusual general feature of the $CuCl_4^{2-}$ spectra is a significant red shift in the band maxima on warming from 10 K to room temperature; this is readily apparent in the spectra of a typical compound containing this ion shown in Figure 1. It was noted that a shift of this magnitude (up to $\sim$950 $cm^{-1}$) is quite incompatible with the simple theory of vibronic intensity stealing, and it was speculated that the breakdown in this model might be due to the unusually low energy ($\sim$65 $cm^{-1}$) of the $\beta_{2u}$ vibration.[5] This normal mode carries the complex from a planar toward a tetrahedral ligand coordination geometry (Figure 9 in Appendix B) and hence effectively produces a small tetrahedral component to the ligand field experienced by the Cu(II) ion at any instant of time. Since a tetrahedral complex has a much smaller d-orbital splitting than a planar complex, a relatively simple explanation of the observed red shift would be that the average ligand field shifts slightly from planar toward tetrahedral with the rise in temperature, due to the population of higher levels of the $\beta_{2u}$ vibration. However, it was shown that this mechanism cannot explain shifts of the observed magnitudes unless the energy of the $\beta_{2u}$ vibration is far lower than the value implied by the temperature dependence of the band intensities.[5]

Two possible alternative mechanisms were proposed for the anomalous red shifts: a significant anharmonicity in the $\beta_{2u}$ vibration in the ground electronic state and/or an equilibrium nuclear geometry in each excited electronic state displaced in the $\beta_{2u}$ coordinate to give a distorted tetrahedral ligand arrangement. [Note that this latter mechanism does not imply that the excited-state potential surface is displaced along the $\beta_{2u}$ coordinate in a manner analogous to the totally symmetric coordinate. The linear terms in the potentials of non totally symmetric vibrations are required by group theory to be zero, a point not always fully appreciated in the literature.[6]] In order to test these ideas we have calculated the parameters defining the band shape of the $^2A_{1g}(z^2) \leftarrow {}^2B_{1g}(x^2-y^2)$ transition of planar $CuCl_4^{2-}$ for various forms of the potential surfaces of the ground and excited electronic states, and the present paper presents the results of these calculations. This transition was chosen because it is relatively well resolved; moreover, in $z$ polarization, theory suggests that the intensity should be derived solely from the single $\beta_{2u}$ vibration, while in $xy$ polarization only modes of $\epsilon_u$ symmetry should be active, so that the dependence of the band shape on the nature of the intensity-inducing vibration may be studied. The simulated spectra have been compared with those observed experimentally for the methadonium salt of the tetrachlorocuprate(II) ion, $(metH)_2CuCl_4$, because for this compound vibrational structure is observed at low temperature on the above electronic transition, which shows that the intensity is derived predominantly via coupling with a single *ungerade* vibration in each polarization,

* To whom correspondence should be addressed.

(1) Lever, A. B. P. *Inorganic Electronic Spectroscopy*, 2nd ed.; Elsevier: Amsterdam, 1984.
(2) (a) Albrecht, A. C. *J. Chem. Phys.* **1960**, *33*, 156. (b) Herzberg, G. *Electronic Spectra and Electronic Structure of Polyatomic Molecules*; Van Nostrand: New York, 1966.
(3) (a) Patterson, H. H.; Godfrey, J. J.; Khan, S. M. *Inorg. Chem.* **1972**, *11*, 2872. (b) Harrison, T. G.; Patterson, H. H.; Godfrey, J. J. *Inorg. Chem.* **1976**, *15*, 1291. (c) Yersin, H.; Otto, H.; Zink, J. I.; Gliemann, G. *J. Am. Chem. Soc.* **1980**, *102*, 951.
(4) Hitchman, M. A.; Cassidy, P. J. *Inorg. Chem.* **1979**, *18*, 1745.
(5) McDonald, R. G.; Hitchman, M. A. *Inorg. Chem.* **1986**, *25*, 3273.
(6) Ballhausen, C. J. *Semi-empirical Methods of Electronic Structure Calculation, Part B: Applications*; Segal, G. A., Ed.; Plenum: New York, 1977; Figure 7, p 159.

0020-1669/87/1326-3205$01.50/0 

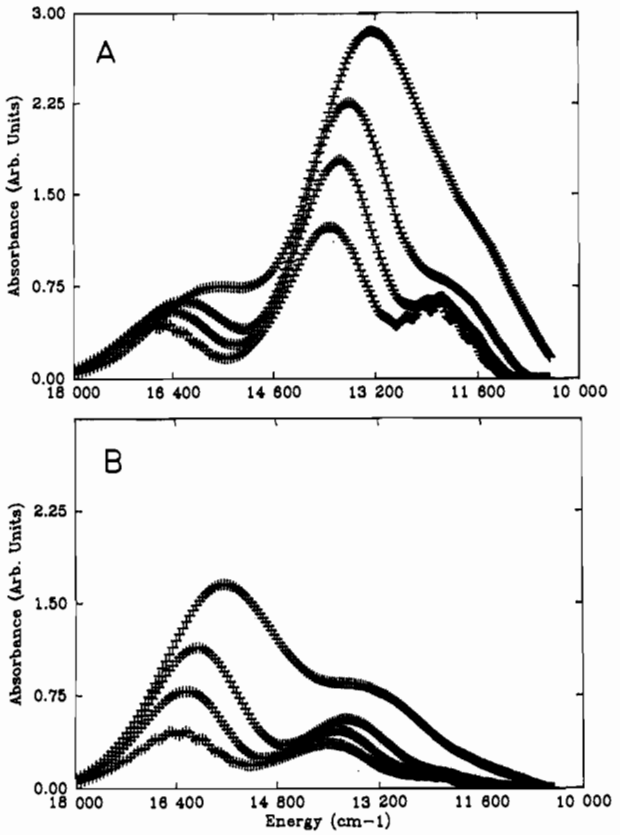


**Figure 1.** Electronic spectrum of the (100) crystal face of (methadonium)$_2$CuCl$_4$ at, in order of increasing intensity, 10, 70, 140, and 265 K, with the electric vector parallel to (A) the *b* and (B) the *c* crystal axes.

greatly simplifying the analysis. The bands due to the other electronic transitions show similar behavior (Figure 1); while it seems likely that this is caused by mechanisms similar to those discussed in the present paper, this has not been investigated quantitatively. In the case of the low energy $^2B_{2g}(xy) \leftarrow {}^2B_{1g}(x^2 - y^2)$ transition, this is too poorly resolved at high temperature to warrant detailed analysis (Figure 1), while for the $^2E_g(xz,yz) \leftarrow {}^2B_{1g}(x^2 - y^2)$ transition the presence of a possible Jahn–Teller distortion in the excited state precludes any simple treatment.

### Theoretical Relationships Defining the Band Shape and Intensity of an Electronic Transition

The vibronic spectrum of a polyatomic system of $N$ atoms depends upon transitions between the ground and excited potential surfaces in an $n = 3N - 6$ dimensional hyperspace. Assuming that the normal coordinates are parallel in the ground and excited states, so that there may be a displacement but no rotation of the normal coordinates (i.e. that no Dushinsky effect is present[7]), the total band shape is a convolution of band shapes attributable to each normal mode taken separately.[8]

The intensity of a transition between the adiabatic wave functions, $|\Psi_g i_1 i_2 i_3 \ldots\rangle$ and $|\Psi_e j_1 j_2 j_3 \ldots\rangle$, where $\Psi_g$ and $\Psi_e$ are the ground and excited electronic states and $i_1, i_2, \ldots$ define the vibrational quantum numbers of the 1st, 2nd, ... normal modes, is then[9]

$$I(i_1,i_2,\ldots;j_1,j_2,\ldots) \propto |\langle i_1,i_2,\ldots,|M_{ge}(Q)|j_1 j_2 \ldots\rangle|^2 \quad (1)$$

where

$$M_{ge}(Q) = \langle \Psi_g(Q)|e_p \textstyle\sum r_p|\Psi_e(Q)\rangle \quad (2)$$

is the electronic transition moment in the electric dipole approximation. Equation 2 can be expanded about the equilibrium nuclear geometry $Q_O$ in terms of the normal coordinates:

$$M_{ge}(Q) = \sum_n M_{ge}(Q_{On}) + \sum_n (\partial M(Q)|\partial Q_n)_O Q_n + \ldots$$
$$= \sum_n M_{ge}{}^n(Q_n) \quad (3)$$

The first term of the expansion is zero for parity-forbidden transitions such as those considered here. Substituting (3) into (1) and letting $k$ of the normal modes be responsible for inducing intensity (i.e. $M_{ge}(Q_k) \neq 0$) yield the relationship

$$I(i_1,i_2,\ldots;j_1,j_2,\ldots) \propto \sum_k^{\text{inducing}} |\langle i_k|M^k(Q_k)|j_k\rangle|^2 \prod_{l\neq k} |\langle i_l|j_l\rangle|^2 \quad (4)$$

The total intensity of the transition is now found by summing over all vibrational quantum numbers in all normal modes of the initial and final states, where a temperature factor is included for the initial occupation of the states:

$$I_{TOT}(T) \propto \sum_i \sum_j \sum_k P_i(T)|\langle i_k|M^k(Q_k)|j_k\rangle|^2 \prod_{l\neq k} P_i^l(T)|\langle i_l|j_l\rangle|^2$$
$$\propto \sum_k I_k(T) \prod_{l\neq k} I_l(T) \quad (5)$$

The intensity due to the $k$th inducing mode, the inducing overlap, is given by

$$I_k(T) \propto \sum_i P_i^k(T) \sum_j |\langle i_k|M(Q_k)|j_k\rangle|^2 \quad (6)$$

while the noninducing overlap is given by

$$I_l(T) = \sum_i P_i^l(T) \sum_j |\langle i_l|j_l\rangle|^2 \quad (7)$$

These overlaps can be evaluated either in the harmonic approximation, in which case analytic formulas can be derived, or by the variational method if nonharmonic potentials are used. The temperature factors

$$P_i^n(T) = \exp(-\epsilon_i^n/kT)/\sum_i \exp(-\epsilon_i^n/kT) \quad (8)$$

give the fractional Boltzmann population of the $i$th vibrational level of energy $\epsilon^n$ in the $n$th normal mode. If the ground state is harmonic, (8) becomes

$$P_i^n(T) = \exp(-ih\nu_n/kT)[1 - \exp(-h\nu_n/kT)] \quad (9)$$

The summation in (7) will always be unity, meaning that the noninducing overlaps contribute nothing to the intensity in (5). However, in the expressions for the mean energy and half-width of a transition given below, additional terms are to be included in this summation that will then differ from 1.0.

Equation 5 gives a relative rather than an absolute intensity, and it is customary to normalize the intensity at 0 K to 1.0:[10]

$$\sum_k I_k(0) = 1.0 \quad (10)$$

The intensity of a spectrum is the integrated absorption curve or zeroth moment of the spectrum. The other temperature-dependent quantities of interest are the mean energy and half-width of the transition, which are related to the first and second moments, respectively. In the present case the band maximum (or mode) of the spectrum will equal the mean energy (since the spectrum to be analyzed, to a good approximation, has a Gaussian line shape), and this is given by[11]

$$E(T) = E_1 + E_2 + E_3 + \ldots \quad (11)$$

where $E_n = I_n(T)\Delta\epsilon_{ij}{}^n/(I_n(T))$ and $\Delta\epsilon_{ij}{}^n = \epsilon_j{}^n - \epsilon_i{}^n$ is the energy difference between the states $|j_n\rangle$ and $|i_n\rangle$.

The analogous relationship for the half-width (full width at half-height) is

$$H(T) = H_1 + H_2 + H_3 + \ldots \quad (12)$$

where $H_n = 2[2(\ln 2)I_n(T)(\Delta\epsilon_{ij}{}^n - E_n)^2/(I_n(T))]^{1/2}$. Here, $E_n$ is given in (11) above, and in both (11) and (12) the $I_n(T)$ terms

(7) Dushinsky, F. *Acta Physicochim. URSS* **1937**, *7*, 551.
(8) O'Brien, M. C. M. *Vib. Spectra Struct.* **1981**, *10*, 321; 323–336.
(9) Roche, M.; Jaffe, H. H. *Chem. Soc. Rev.* **1976**, *5*, 165.
(10) Lohr, L. L. *J. Am. Chem. Soc.* **1970**, *92*, 2210.
(11) Markham, J. J. *Rev. Mod. Phys.* **1959**, *31*, 956.

are given by either (6) if the mode is "active" or (7) if it is not. It is important to realize that the terms subscripted $i$ and $j$ in (11) and (12) are to be included in the summation over $i$ and $j$ in (6) and (7). It can be seen that the denominators of these equations will be equal to unity if the mode is "inactive" ($n \neq k$). Again it is pointed out that while (5) only gives the *relative* intensity, (11) and (12) give the *absolute* mean energy and half-width, respectively.

**Harmonic Approximation.** Analytic formulas for the temperature dependence of the three quantities of interest, the intensity, band shift, and half-width in the harmonic approximation, assuming a linear dependence of the electronic transition moment on $Q$, are given below.

**I. Intensity.** This is given by[2a]

$$I(T) = \sum_k I_k(0) \coth X_k \tag{13}$$

where $X_k = (h\nu_k/2kT)$. Note that if (3) contains quadratic terms, then[12]

$$I(T) = \sum_k I_{1k}(0) \coth X_k + I_{2k}(0) \coth^2 X_k \tag{14}$$

where $I_{1k}$ and $I_{2k}$ are determined by the relative size of the coefficients in (3). Equations 13 and 14 assume a harmonic ground state for the inducing mode while the excited state may take any form. The ground and excited states of the noninducing modes may also be an arbitrary function of the normal coordinates.

**II. Band Shift.** The shift of the band maximum from that expected for a pure vertical electronic transition is given by[11,13]

$$E(T) = \sum_k h\nu_k \tanh X_k + 0.25 \sum_l h\nu_l(\delta_l - 1) \coth X_l \tag{15}$$

where $\delta_l = (h\nu'_l/h\nu_l)^2$, $h\nu'_l$ being the excited-state frequency.

Equation 15 assumes that the potentials of all modes in both ground and excited states are harmonic. In addition, the $k$ inducing modes must have their excited-state potentials undisplaced and be of the same frequency as the ground state. The $l$ noninducing modes may have their excited-state potentials displaced or have frequencies that differ from those in the ground state.

**III. Half-Width.** The variation in half-width is given by[11,13]

$$H(T) = \sum_k 2h\nu_k(2(\ln 2))^{1/2} \operatorname{sech} X_k + \sum_l 2h\nu_l[2(\ln 2)(S\delta_l \coth X_l + (\delta_l - 1)^2(\coth^2 X_l)/8)]^{1/2} \tag{16}$$

where $S = \Delta S^2\delta_l/2$ is the Huang–Rys factor,[11] $\Delta S$ is the displacement of the surfaces, and all other definitions are as before. Equation 16 has been derived by assuming the same conditions as given for (15).

The first summation over the inducing modes, in (15) and (16), have apparently not previously appeared in the literature. Their derivation is given in Appendix A. Some general comments concerning the above expressions may now be made.

(i) No use has yet been made of symmetry. In general, the inducing modes may be of any symmetry (even totally symmetric) as long as other transitions of suitable symmetry are available for mixing. In the present centrosymetric case all inducing modes are required by group theory to be non totally symmetric and displaced. The assumption of undisplaced potentials for the inducing modes in the derivation of (15) and (16) is then justified.

(ii) The intensity in (13) and (14) is due entirely to the inducing modes.

(iii) The band maximum shift due to the inducing modes $k$ goes from $h\nu_k$ near absolute zero (0 K) to 0 at high temperature ($\infty$ K); i.e. at low temperature, only the $0 \rightarrow 1$ transition will be observed, while at high temperature a nearly equal number of $n \rightarrow n+1$ and $n \rightarrow n-1$ transitions will occur, which will average to a mean of zero. A maximum band shift due to an increase in temperature of less than $h\nu_k$ is therefore expected as a result of the inducing modes.

(iv) Noninducing modes will only produce a shift in band maximum with temperature if the frequencies are different in the ground and excited states.

(v) The half-width due to the inducing modes will grow from 0 (0 K) to $2(2 \ln 2)^{1/2}h\nu_k$ at high temperature. The noninducing modes, however, will give a finite bandwidth at 0 K, the most important factor being the displacement of the surfaces $\Delta S$.

Equations 13–16 are valid, of course, only under the conditions in which the approximations made in their derivation are valid. In particular, anharmonicity of the vibrations can cause significant deviations from the behavior predicted by the expressions. Dreybrodt and Fussgaenger[14] have derived an expression for the temperature dependence of the intensity for an oscillator with quartic anharmonicity using perturbation theory. However, this is very cumbersome and has only limited validity. A more profitable approach for an anharmonic potential is the variational method outlined below.

**Variational Calculations.** To use the general expressions (5), (11), and (12), overlaps (6) and (7) must be evaluated and the energies of the vibronic levels are required. For an adiabatic potential surface of arbitrary shape, this is most easily done by the variational method, explained in detail by Lohr.[10]

For the present calculations the potentials of the ground and excited states are expressed as the sum of a fourth-order polynomial and a Gaussian function. The vibrational Hamiltonian is then

$$H = -0.5\partial^2/\partial\xi^2 + V(\xi);\ V(\xi) = \sum_{p=0}^{4} a_p\xi^p + \alpha \exp(-\beta\xi^2) \tag{17}$$

Here, $\xi$ is a dimensionless coordinate related to the symmetry coordinates by[15]

$$S = \xi/x;\ x = 1.722 \times 10^{-3}(M h\nu)^{1/2}\ \text{pm}^{-1} \tag{18}$$

where $M$ is the inverse of the element of the **G** matrix in amu appropriate to the normal coordinate (see Appendix B) and $h\nu$ is the unit of energy in $cm^{-1}$ for (17). The ground- and excited-state wave functions are expanded in a basis of harmonic oscillator functions that are characterized by a harmonic energy $h\nu$.

The matrix elements of (17) in this basis are easily evaluated by published methods.[16] After diagonalization of the secular equation with standard techniques,[17] the energies are obtained in (nonintegral) units of $h\nu$ and the wave functions $|i\rangle$,$|j\rangle$ as a linear combination of the harmonic basis functions $\phi_n$:

$$|i\rangle = \sum_{n=0}^{N} c_{ni}\phi_n;\ |j\rangle = \sum_{n=0}^{N} c_{nj}\phi_n \tag{19}$$

Overlaps (6) and (7) can then be evaluated:[10]

$$\langle i|j\rangle = \sum_{n=0}^{N} c_{ni}c_{nj} \tag{20}$$

$$\langle i|\xi|j\rangle = \sum_{n=1}^{N} (n/2)^{1/2}[c_{ni}c_{n-1j} + c_{n-li}c_{nj}] \tag{21}$$

$$\langle i|\xi^2|j\rangle = \sum_{n=2}^{N} 0.5[(n(n-1))^{1/2}(c_{ni}c_{n-2j} + c_{n-2i}c_{nj})] + \sum_{n=0}^{N} (n + \tfrac{1}{2})c_{ni}c_{nj} \tag{22}$$

Having these transition probabilities between all possible levels,

(12) Fussgaenger, K.; Martienssen, W.; Bilz, H. *Phys. Status Solidi B* **1965**, *12*, 383.
(13) Prassides, K.; Day, P. *J. Chem. Soc., Faraday Trans. 2* **1984**, *80*, 85. Note: There is a misprint in eq 3 of this paper. See eq 16 of the present paper for the correct expression.
(14) Dreybrodt, W.; Fussgaenger, K. *Phys. Status Solidi B* **1966**, *18*, 133.
(15) Cyvin, S. J. *Molecular Vibrations and Mean Square Amplitudes*; Elsevier: Amsterdam, 1968.
(16) (a) Shaffer, W. H.; Krohn, B. J. *J. Mol. Spectrosc.* **1976**, *63*, 323. (b) Chan, S. I.; Stelman, D. *J. Chem. Phys.* **1963**, *39*, 545.
(17) Smith, B. T.; Boyle, J. M.; Garbow, B. S.; Ikebe, Y.; Klema, V. C.; Moler, C. B. In *Lecture Notes in Computer Science*, 2nd ed.; Springer: Berlin, 1976; Vol. 6, "EISPACK guide".

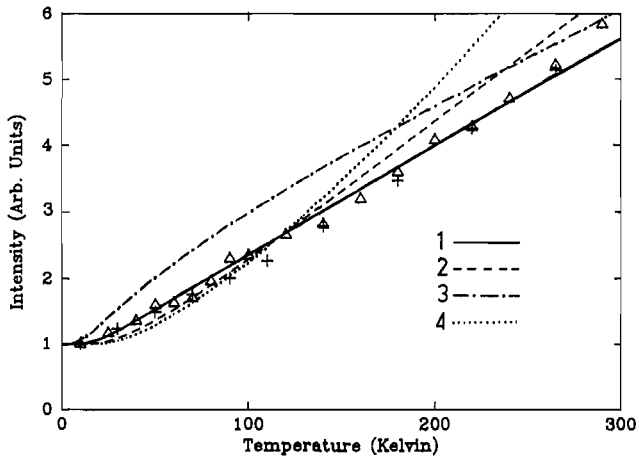


**Figure 2.** Calculated and observed temperature dependence of the intensity of the $^2A_{1g}(z^2) \leftarrow {}^2B_{1g}(x^2 - y^2)$ transition in $z$ polarization. The triangles and crosses refer to data measured by using two different crystals. The calculated curves were obtained by using the following $\beta_{2u}$ potentials: (1) potential given by equation (23); (2) harmonic potential with a vibrational energy of 65 $cm^{-1}$; (3) highly anharmonic potential chosen to fit experiment at 0 and 300 K; (4) second-order dependence of the transition moment, calculated by using a harmonic potential with $h\nu$ = 75 $cm^{-1}$ and $I_{01}$ = 0.9 and $I_{02}$ = 0.1 in (14). Potentials 1–3 are shown in Figure 3.

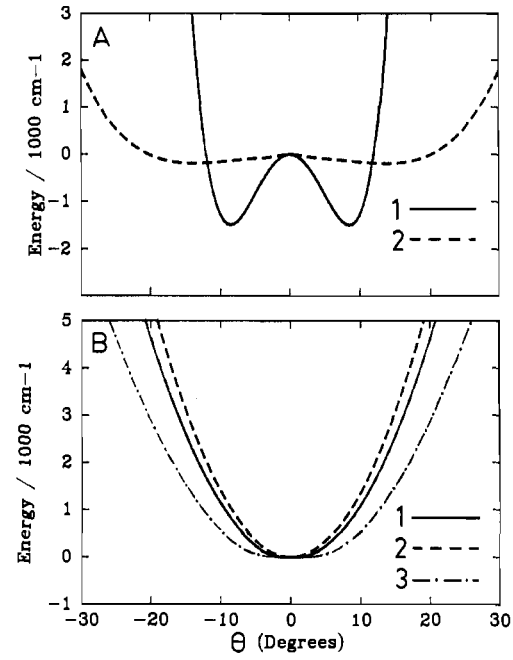


**Figure 3.** Potential surfaces along the $\beta_{2u}$ coordinate: (A) excited-state potentials with curve 1 being the (nonunique) potential that fits the experimental data and curve 2, being the potential obtained by using the angular overlap model; (B) ground-state potentials, defined as given in Figure 2.

the spectrum may either be simulated or, more conveniently, subjected to a moments analysis. For the latter, the summation over all such overlaps, including both temperature factors for the ground state and any other factors dependent on $i$ or $j$ from (10) or (11), gives the desired quantities.

The size of the basis $N$ that is required is determined largely by the temperature factor (eq 8). Enough energy levels must be included in the summation to make every temperature factor converge. This is most easily done by increasing the basis size until the temperature factors become constant. Basis sizes of about 60 were generally found to be sufficient in the present case.

### Analysis of the $^2A_{1g}(z^2) \leftarrow {}^2B_{1g}(x^2 - y^2)$ Transition of $(metH)_2CuCl_4$

The experimental electronic spectra of the planar $CuCl_4^{2-}$ ion in this compound show a large temperature dependence (Figure 1). It has been shown by Lohr[18] that the variation of the band *intensity* with temperature is related only to the ground-state potential surfaces, assuming that the transition moment has a linear dependence on the inducing coordinates. Fixing the potential surfaces of the ground state in this manner greatly simplifies the analysis of the shift in band maximum with temperature, as it means that this can be considered simply in terms of possible potential surfaces of the excited electronic state.

**Temperature Dependence of the Intensity: Influence of the Ground-State Potential Surfaces.** On going from 10 to 295 K, the spectrum increases significantly in intensity, as expected for a parity-forbidden electronic transition (the chromophore is situated on a crystallographic inversion center, and so is rigorously centrosymmetric). When the electric vector is parallel to the $c$ crystallographic axis of $(metH)_2CuCl_4$, it is aligned almost exactly with the molecular $z$ axis of the planar $CuCl_4^{2-}$ ion, and in this polarization only the out-of-plane $\beta_{2u}$ mode induces intensity into the transition of interest. As shown in a previous analysis, the variation of the band intensities of the observed spectra derived by Gaussian analysis may be explained reasonably well by using the simple "coth rule" given by eq 13, assuming a value of 65 $cm^{-1}$ for the energy of the $\beta_{2u}$ mode.[5] However, as may be seen from the plot in Figure 2, the experimental intensities rise more rapidly than predicted at low temperature and tend to fall away from the expected increase at higher temperatures.

Two mechanisms have been suggested for deviations from the simple coth rule of intensity stealing. Ferguson[19] has proposed that the $n \rightarrow n \pm 1$ transitions of an inducing mode may become more intense for increasing $n$ than is suggested by the coth rule. This is turn implies that the electronic transition moment should be expanded to second order, which yields the quadratic coth rule given in (14) above. However, the application of this formula leads to a relationship in which the intensity increases more rapidly at higher temperatures than is predicted by the simple rule (Figure 2), the opposite of the behavior observed experimentally, so that this explanation cannot be correct in the present system. Alternatively, Englman[20] has suggested that anharmonicity of the inducing vibration may influence the temperature dependence of band intensities, and a similar proposal has recently been made by Bacci.[21] The variation of the band intensity as a function of temperature was calculated by the variational method described above for a range of anharmonic potentials. To explain the observed behavior at low temperature the basic energy of the vibration must be less than the 65 $cm^{-1}$ suggested by the simple coth relationship, while the deviation at high temperature implies that the form of the anharmonicity is to cause an increase in the slope of the potential surface as a function of the normal coordinate. It may be noted that a similar type of anharmonicity was proposed by Englman to explain the temperature dependence of the optical spectrum of $Ni(H_2O)_6^{2+}$.[20] A ground-state potential of the form

$$V(\xi) = 0.5\xi^2 + \exp(-0.5\xi^2);\ h\nu = 60\ cm^{-1} \qquad (23)$$

produces satisfactory agreement with experiment (Figure 2). This surface is compared with the harmonic potential corresponding to an energy of 65 $cm^{-1}$ in Figure 3, from which it may be seen that the anharmonicity is quite modest.

Because of the importance of defining the ground-state potential surface as accurately as possible in considering the cause of the shift in band maximum with temperature, the effect of a highly anharmonic ground-state potential on the variation of the intensity with temperature was considered. Various surfaces were investigated, each chosen to produce a ratio of the intensity at 295 K to that at 10 K in agreement with that observed experimentally.

(18) Lohr, L. L. *J. Chem. Phys.* **1969**, *50*, 4596.

(19) Ferguson, J. *Prog. Inorg. Chem.* **1970**, *12*, 159.
(20) Englman, R. *Mol. Phys.* **1960**, *3*, 23.
(21) Bacci, M. *Chem. Phys.* **1984**, *88*, 39.

However, these invariably implied a variation over the intervening temperatures differing drastically from experiment. A typical plot, obtained by using the potential surface 3 in Figure 3, is shown in Figure 2. It should also be noted that the root-mean-square amplitude of the $\beta_{2u}$ mode at room temperature that is implied by the potential given by (23) (with each Cu–Cl bond making an angle of $\sim 2.7°$ with the $xy$ plane) is in good agreement with the thermal ellipsoids deduced from the X-ray crystal structure analysis ($\sim 3°$), which would not be the case for the highly distorted potential surface in Figure 3.

When the electric vector is parallel to the $b$ crystal axis of $(metH)_2CuCl_4$, this produces an almost pure $xy$ molecular spectrum. In this polarization the $^2A_{1g}(z^2) \leftarrow {}^2B_{1g}(x^2 - y^2)$ transition is induced by vibrations of $\epsilon_u$ symmetry. The low-temperature spectrum consists of two progressions, one far more intense than the other. A previous analysis has shown that the observed temperature dependence of the intensity is in good agreement with the dominant progression being due to coupling with the $\epsilon_u$ in-plane bend of energy $\sim 178$ cm$^{-1}$ (the corresponding stretching vibration, of energy $\sim 290$ cm$^{-1}$ is for some unknown reason apparently completely inactive[5]). The minor progression (contributing $\sim 6\%$ to the intensity at 10 K) is due to coupling with what is presumably a lattice mode of energy $\sim 80$ cm$^{-1}$. This means that the "effective" energy of the $\epsilon_u$ mode in inducing intensity is $\sim 165$ cm$^{-1}$, and the following "effective" potential was found to give good agreement with the temperature dependence of the band intensity in $xy$ polarization

$$V(\xi) = 0.5\xi^2 + 2\exp(-0.25\xi^2);\ h\nu = 165\ \text{cm}^{-1} \qquad (24)$$

with a slight anharmonicity correction being added to take into account the effect of the low-energy lattice vibration.

**Temperature Dependence and Polarization Behavior of the Band Maxima: Influence of the Excited-State Potential Surfaces.** Perhaps the most unusual feature of the electronic spectrum of the planar $CuCl_4^{2-}$ ion is the dramatic shift to lower energy of the band maxima as the temperature is raised from 10 to 295 K (Figure 1). For the band under consideration this shift is somewhat greater in $z$ polarization ($\sim 950$ cm$^{-1}$) than in $xy$ polarization ($\sim 800$ cm$^{-1}$). It is also noteworthy that the band maximizes at significantly higher energy in $xy$ than in $z$ polarization, the energy difference being $\sim 250$ cm$^{-1}$ at low temperature, with this approximately doubling by room temperature. Moreover, essentially identical behavior has been reported[5] for this complex in the similar compound $(creatininium)_2CuCl_4$, so that these features are apparently a general characteristic of the spectrum of the complex.

The only mode in which the excited-state potential surface may be displaced with respect to the ground state is that of $\alpha_{1g}$ symmetry, and it is apparent that the observed progressions at low temperature are indeed in this vibration. As discussed in a previous publication,[5] the band shape is consistent with a displacement in the excited electronic state of 21.2 pm in the minimum of this mode, corresponding to a lengthening of 10.6 pm in each Cu–Cl bond. As expected from the increase in bond lengths, the observed progressional energy of 265 cm$^{-1}$ is slightly less than the ground-state energy of the $\alpha_{1g}$ vibration, 275 cm$^{-1}$.[5]

If it is assumed that, with the exception of the $\alpha_{1g}$ vibration, the excited-state potential surfaces are identical with those in the ground state, then (15) may be used to estimate the variation of the band maximum as a function of temperature. The shifts calculated in this way are far smaller than those observed experimentally, as may be seen from the plots shown in Figure 4; in these, the electronic origin has been arbitrarily chosen to make the band maximum in $z$ polarization agree with experiment. Here, the shifts are mainly due to the "hot" bands associated with the inducing modes. The red-shift tends toward $h\nu$ at high temperature, where $h\nu$ is the energy of the inducing mode (eq 15). The difference in the frequency of the $\alpha_{1g}$ vibration in the ground and excited state also makes a small contribution. The energy difference between the band maxima in $xy$ and $z$ polarization is also too small and tends to decrease with the increase in temperature, the opposite of experimental observation. It has been suggested

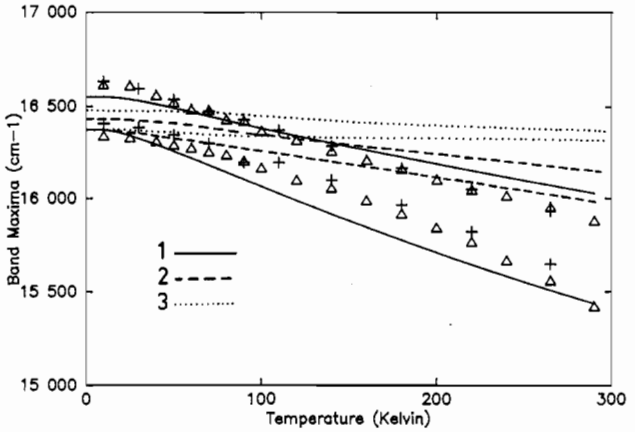


**Figure 4.** Temperature dependence of the band maxima. The higher energy experimental points and calculated curves refer to $xy$ polarization, and the lower energy refers to $z$ polarization: curve 1, obtained with the ground- and excited-state potentials of curves 1 in Figure 3; curve 2, obtained by using the excited-state potential derived from the angular overlap model, curve 2 in Figure 3; curve 3, obtained by using harmonic ground- and excited-state potentials.

by Englman that the red shift in the band maxima of $Ni(H_2O)_6^{2+}$ is due to an effective increase in the metal–ligand bond length with rise in temperature, this being quantified by a significant anharmonicity in the $\alpha_{1g}$ vibration.[20] Such a mechanism is clearly impossible in the present case, both because of the high energy of this mode and because no anharmonicity is observed in the band structure of the electronic transitions. Moreover, the energy of the peak due to the $\alpha_{1g}$ vibration observed in the Raman spectrum of compounds containing planar $CuCl_4^{2-}$ does not shift when they are cooled.[22]

Given that the ground-state potential surfaces of the inducing modes are apparently quite normal (see preceding section), it seems reasonable to conclude that the anomalous behavior of the electronic bands of planar $CuCl_4^{2-}$ is related to the way in which these surfaces differ in the excited electronic states. Each electronic transition involves excitation from an approximately nonbonding orbital to an antibonding orbital, and as mentioned above, a displacement in the $\alpha_{1g}$ mode occurs because of this. In general terms, the longer metal–ligand bonds in each excited state suggest a reduction in the vibrational force constants compared with the values in the ground state. An approximate estimate of the required potential surfaces may be obtained by adding to each ground-state potential the variation in the energy of the excited state as a function of that particular normal coordinate. This procedure is directly analogous to the well-established method of deducing the potential surface of a molecule that has undergone a Jahn–Teller distortion, where the change in electronic energy as a function of the Jahn–Teller active coordinate is added to the potential surface expected in the absence of this effect. It may be noted that, except for $\alpha_{1g}$ modes, symmetry arguments dictate that for a nondegenerate electronic state the change to every vibrational potential must be a nonlinear function of the normal coordinate. An approach of this kind has recently been used to successfully estimate the change in bond length that generally accompanies a rearrangement of the d electrons in a transition-metal complex and the displacement in the $\epsilon_g$ coordinate in Jahn–Teller active systems.[23]

The form of the symmetry coordinates of the planar $CuCl_4^{2-}$ ion are shown in Appendix B. As discussed in Appendix B, the ligand displacements along the $\beta_{1g}$ and $\epsilon_u$(s) stretching coordinates will not cause significant changes in the d-orbital energies, apart from removing the degeneracy of the $^2E_g(d_{xz,yz})$ state. This is because as two ligands approach the metal, their effect is approximately counterbalanced by the other two moving away. Although attention is focused here on just one excited state,

(22) Cassidy, P. J.; Hitchman, M. A.; McDonald, R. G., unpublished work.
(23) Deeth, R. J.; Hitchman, M. A. *Inorg. Chem.* **1986**, *25*, 1225.

**Table I.** Parameters Defining Excited-State Potential Surfaces Derived by Using the Angular Overlap Model

| | $\alpha_{1g}$ ($\nu_1$) | $\alpha_{2u}$ ($\nu_3$) | $\beta_{2g}$ ($\nu_4$) | $\beta_{2u}$ ($\nu_5$) | $\epsilon_2$ ($\nu_7$) |
|---|---|---|---|---|---|
| $h\nu$,[a] cm$^{-1}$ | 275 | 159 | 181 | 65 | 165 |
| $a_1'$[b] | −3.6385 | 0.0 | 0.0 | 0.0 | 0.0 |
| $a_2'$[b] | 0.4643[c] | 0.2408 | 0.5380 | −0.0632 | 0.3224 |
| $a_4'$[b] | 0.0 | 0.00024 | 0.0012 | 0.00043 | −0.0005 |
| $E(0)$,[d] cm$^{-1}$ | −4.9 | −20.6 | 3.6 | −23.2,[e] −21.3[f] | −23.8,[e] 35.9[f] |
| $E(300)$,[d] cm$^{-1}$ | −8.5 | −56.4 | 9.4 | −129.6,[e] −350.4[f] | −61.2,[e] −111.8[f] |

[a] Fundamental energy of vibration in the ground state. [b] Coefficients defining the excited-state potential. [c] This coefficient produces an excited-state potential having a fundamental energy equal to that observed experimentally; $h\nu$ = 265 cm$^{-1}$. [d] These energies, at 0 and 300 K, are given relative to the energy difference between the ground- and excited-state potential surfaces at the equilibrium nuclear geometry of the ground state. [e] Noninducing. [f] Inducing.

$^2A_{1g}(z^2)$, for completeness the change in all the d-orbital energies as a function of displacements in each of the bending vibrations were calculated. The appropriate angular overlap expressions were used to parametrize the metal–ligand interactions, with the bonding parameters being defined by the excited-state energies of the limiting planar ion. Details are given in Appendix B, as are plots of the d-orbital energy variations as a function of each normal coordinate (Figure 10). The optimum fourth-order polynomial to describe each variation over the range ±15° was determined by a least-squares procedure, and this was added to the appropriate ground state potential to produce excited-state potential functions defined by the coefficients indicated in Table I.

For every mode except that of $\beta_{2u}$ (and $\alpha_{1g}$) symmetry the potential in the $^2A_{1g}(z^2)$ excited state is calculated to be similar to that in the ground state except for the expected lowering of the force constant. This is because in each case the d-orbital energy variation obeys a relationship that is dominated by the quadratic coefficient (Table IV), the linear coefficient being found to be zero, in agreement with the requirements of group theory. However, the potential surface calculated for the $\beta_{2u}$ mode in the excited state is quite different from that in the ground state, having two shallow minima, of depth ~140 cm$^{-1}$, located at $\theta = \pm\sim 14°$. This implies that the destabilization with respect to this normal coordinate that accompanies the electronic excitation is marginally more than enough to overcome the ground-state force constant, so that the equilibrium nuclear geometry in the excited state actually corresponds to two equivalent distorted tetrahedral ligand arrangements. The reason why this particular mode shows such unusual behavior is due partly to its very small force constant in the ground state and partly to the high sensitivity of the d-orbital energies to a change in this normal coordinate (Figure 10). The calculated excited-state potential surface as a function of the $\beta_{2u}$ coordinate is compared with those of the ground state in Figure 3. It should be noted that, again in agreement with the requirements of group theory, the slope of the calculated excited-state potential surface is zero at $\theta = 0°$.

The temperature dependence of the $^2A_{1g}(z^2)$ band maximum, obtained by using the calculated potential surfaces of the excited state, is shown in Figure 4. Agreement with experiment is still not good, though as far as the red shift is concerned it is a little better than was obtained by assuming excited-state potential surfaces identical with those in the ground state. The relative contributions of the various different modes to the change in band maximum position from that predicted by assuming these ground- and excited-state potentials are shown in Table I. From these it may be seen that only the $\beta_{2u}$ and $\epsilon_u$(b) modes make any significant contribution, either to the temperature dependence of the band maximum or to the difference in band maximum between $z$ and $xy$ polarization. Moreover, while the former vibration has a large effect in both polarizations, the latter only contributes significantly to the shift in band maximum when it is the inducing mode ($xy$ polarization).

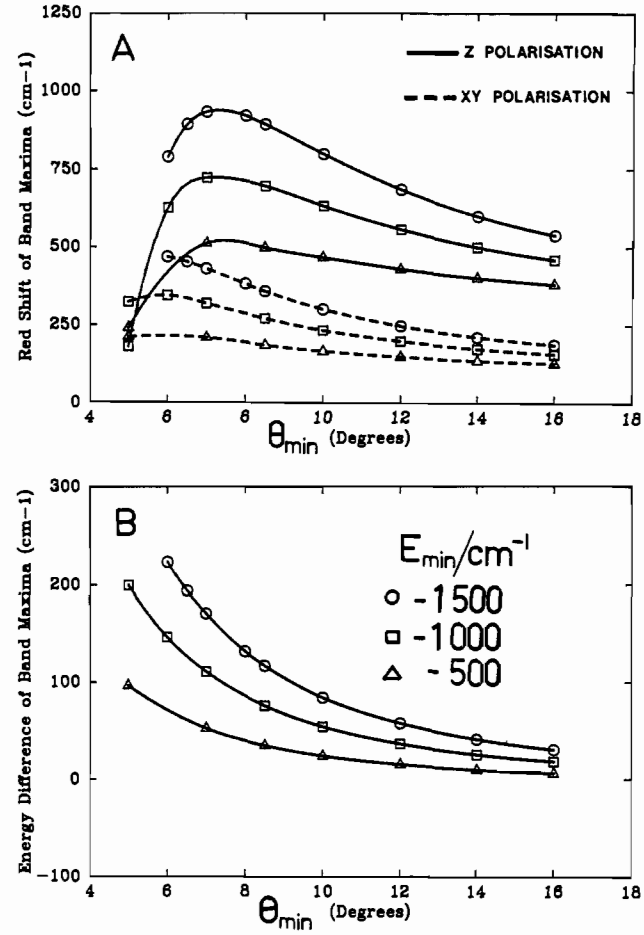


*Figure 5.* Spectral parameters obtained by using various $\beta_{2u}$ potentials, with $\theta_{min}$ and $E_{min}$ defined as in (25): curve A, shift in band maxima; curve B, energy of the band maximum in $xy$ polarization minus that in $z$ polarization.

The dominance of the contribution of the $\beta_{2u}$ vibration to the shift in band maximum with temperature is clearly related to the fact that the potential surface of the excited electronic state differs substantially from that of the ground state in this normal coordinate. It was therefore decided to investigate the sensitivity of the polarization and temperature shifts of the band maximum to the depth ($E_{min}$) and angular displacement ($\theta_{min}$) of the wells in the excited state $\beta_{2u}$ potential surface. These quantities are related in a simple fashion to the coefficients $c_2$ and $c_4$, which define the potential surface (see eq A7 of Appendix B):

$$\theta_{min} = (-c_2/2c_4)^{1/2};\ E_{min} = -(c_2^2/4c_4) \qquad (25)$$

From the plots shown in Figure 5a, it can be seen that a red shift corresponding to those observed experimentally on warming from 10 to 295 K would occur if the minima were much deeper ($E_{min} \simeq 1500$ cm$^{-1}$) than those estimated by using the angular overlap approach and displaced by $\theta_{min} \simeq 8.5°$. As might be expected, and in agreement with observation, the shift is greater in $z$ polarization, where the $\beta_{2u}$ is the inducing mode, than in $xy$ polarization, where it is not. This is because in the former case the calculated overlaps become increasingly more significant, compared with the latter case, as higher vibrational levels of the $\beta_{2u}$ mode are populated in the ground state. The red shift increases as the minima move inward from a large value. Classically, this can be visualized as being due to the vertical transition from the root-mean-square geometry at high temperatures in the ground state cutting the excited-state potential at lower and lower energy as the minima move in.

The effect of the various potentials on the difference in the band maximum in $z$ and $xy$ polarization is shown in Figure 5b. It can be seen that agreement with experiment is obtained with similar values of $E_{min}$ and $\theta_{min}$ to those required to optimize the tem-

perature dependence of the band maximum. This is again a consequence of the fact that the $\beta_{2u}$ mode, in which the excited state has a double minimum, induces intensity in $z$ but not in $xy$ polarization.

While the above potential surface is almost certainly not the only one that would produce the observed features (one with even deeper minima displaced further from planarity would probably do so), the fact that the red shift and the polarization behavior of the $^2A_{1g}(z^2)$ band maximum independently require such a similar excited-state potential surface suggests that the general features of this are likely to be correct. In particular, the large size of the red shift ($\sim$900 cm$^{-1}$) implies that the excited-state potential surface decreases in energy with respect to that of the ground state by about this amount as the average displacement in the $\beta_{2u}$ coordinate increases from the zero-point value of $|\theta| \simeq 1.1°$ to the value at room temperature, confirmed independently by the X-ray crystal structure analysis as $|\theta| = 2.7°$. This requires that the excited-state potential falls steeply over this range, which must produce a surface with double minima such as that pictured in Figure 3. Similar surfaces have been proposed for excited states of other planar complexes. For instance, Ballhausen et al.[24] have suggested a distorted tetrahedral equilibrium nuclear geometry for the $^1B_{2g}(D_{4h})$ state of $Ni(CN)_4^{2-}$, in order to explain the anomalous polarization behavior of the electronic spectrum of this complex. Similarly, Martin et al.[25] have proposed that the lack of vibrational fine structure on the $^1E_g \leftarrow {}^1A_{1g}$ transition of $PtCl_4^{2-}$ may be due to a pseudotetrahedral distortion in the doubly degenerate excited state.

The $CuCl_4^{2-}$ ion is, in fact, particularly likely to undergo a distortion toward a distorted tetrahedral ligand geometry, since this is apparently the preferred stereochemistry of this complex in the absence of lattice forces. The angle $\theta$ is $\sim$25° in lattices with non-hydrogen-bonding counterions, and in noncoordinating solvents.[26] Moreover, one of the compounds that contains planar $CuCl_4^{2-}$ at room temperature undergoes a phase transition to a form containing pseudotetrahedral species at $\sim$69 °C.[27] At first sight it might seem disquieting that the potential surface giving optimum agreement with the spectral behavior differs so substantially from that estimated by using the angular overlap model (Figure 3). However, it should be noted that the latter approach only considers the contribution to the excited-state potential caused by the rearrangement of the d electrons. The vibronic coupling with excited-charge-transfer states is also expected to contribute to the distortion from planarity in the excited d states (in planar $CuCl_4^{2-}$ the lowest charge-transfer states are only $\sim$8000 cm$^{-1}$ above the excited d states[28]). Vibronic coupling with a neighboring excited state has recently been shown to strongly influence the potential surface of an excited state of $SO_2$,[29] and it has also been proposed that the photophysical properties of several nitrogen–heterocyclic and aromatic carbonyl compounds can be attributed to vibronic coupling between nearby $n\pi^*$ and $\pi\pi^*$ excited states.[30]

**Variation of Half-Width with Temperature.** The half-width of the band is due largely to progressions in the $\alpha_{1g}$ vibration. A previous analysis of the relative intensities of the band components yielded an estimate of $\Delta S = 21.2$ pm for the displacement in this mode in the $^2A_{1g}(z^2)$ excited state,[5] and the present simulations of the spectra confirm this.

A moments analysis of the temperature dependence of the half-widths using (16) was actually found to give better agreement with the parameters obtained from Gaussian analysis of the spectra if identical potential surfaces in the ground and excited state were assumed than if the distorted excited-state potentials described above were used. This is because a moments analysis, which calculates the mean width of a line shape, can only be related to the half-width when the line shape is Gaussian.[13] Clearly this is not the case for the non totally symmetric modes, and the use of (12) or (16) will grossly overestimate the contribution of these modes to the half-width of the total band shape. Under these circumstances, rather than consider the half-widths as such, it is better to compare simulated spectra with the line shapes observed at various temperatures.

**Simulation of the Spectra.** If the observed spectral curves at low temperature are considered to be progressions in the $\alpha_{1g}$ mode, built on a single vibronic origin, then the ground- and excited-state potentials in this symmetry coordinate in pm are given by

$$V_g(S_{\alpha 1g}) = 3.975 S_{\alpha 1g}^2$$

$$V_e(S_{\alpha 1g}) = 3.690 S_{\alpha 1g}^2 - 156.5 S_{\alpha 1g} \qquad (26)$$

These correspond to harmonic potentials displaced by $\Delta S = 21.2$ pm, with vibrational energies of 275 and 265 cm$^{-1}$ for the ground and excited states, respectively. In the dimensionless units appropriate to a variational calculation with the energy units $h\nu = 275$ cm$^{-1}$, these potentials are

$$V_g(\xi) = 0.5\xi^2$$

$$V_e(\xi) = 0.464\xi^2 - 3.347\xi \qquad (27)$$

The appropriate mass for this vibration is that of one ligand, and the relationship between the "force constants" is given in (18).

Ideally, the spectra should be simulated by calculating the vibronic overlaps between the complex in every combination of all the vibrational levels of the ground and excited state at each temperature under consideration, with weighting factors being introduced to account for the Boltzmann distribution over the ground-state levels. In practice, such a procedure would be extremely time consuming, and only the potential surfaces of the $\alpha_{1g}$ mode, and the inducing vibrations, $\beta_{2u}$ in $z$ polarization and $\epsilon_u$ in $xy$ polarization, have been considered here. The first of these provides the band envelopes, while the second two provide the intensity and energy of each vibronic origin upon which the bands are built. The effects of the noninducing modes on the energies of the transitions can be quite substantial, particularly that of the $\beta_{2u}$ vibration in $xy$ polarization, and these have been included in the calculations. The lines are given a finite half-width to produce optimum agreement with the low-temperature spectrum, and this is kept constant in simulating the higher temperature spectra; the consequences of this particular assumption are considered below. It was found that an identical basic half-width (full width at half-height of $\sim$270 cm$^{-1}$), could be used for both polarizations. The electronic origin was chosen to reproduce the low-temperature spectrum in $z$ polarization.

The spectra at four temperatures between 10 and 295 K, simulated by assuming the excited-state potential surfaces derived with the angular overlap model, are compared with those observed experimentally in Figure 6a,b. Here, the intensity due to the $^2E_g(xz,yz) \leftarrow {}^2B_{1g}(x^2 - y^2)$ transition has been subtracted from the experimental spectra. Because of the relative weakness of the $^2A_{1g}(z^2) \leftarrow {}^2B_{1g}(x^2 - y^2)$ transition in $xy$ polarization (Figure 1a), the subtraction procedure produced anomalous effects in the region between the two higher energy bands, so in this case the experimental spectra are represented by the best-fit Gaussian curves to the data. While the intensity variations are reproduced well, as these are decided by the ground-state potential surfaces, the pronounced deviation of the band position from that observed experimentally at high temperatures is readily apparent. It is also noteworthy that the vibrational fine structure is predicted to die away less rapidly with increasing temperature than is the case experimentally. The spectra simulated by using an excited state potential surface with double minima ±8.5° from the saddle point, each with a depth of 1500 cm$^{-1}$, are shown in Figure 7a,b. For the spectrum in $z$ polarization agreement is satisfactory in all

(24) Ballhausen, C. J.; Bjerrum, N.; Dingle, R.; Eriks, K.; Hare, C. R. *Inorg. Chem.* **1965**, *4*, 514.
(25) Martin, D. S., Jr.; Tucker, M. A.; Kassman, A. J. *Inorg. Chem.* **1965**, *4*, 1682.
(26) Harlow, R. L.; Wells, W. J.; Watt, G. W.; Simonsen, S. H. *Inorg. Chem.* **1975**, *14*, 1768.
(27) Harlow, R. L.; Wells, W. J.; Watt, G. W.; Simonsen, S. H. *Inorg. Chem.* **1974**, *13*, 2106.
(28) Desjardins, S. R.; Penfield, K. W.; Cohen, S. L.; Musselman, R. L.; Solomon, E. I. *J. Am. Chem. Soc.* **1983**, *105*, 4590.
(29) Innes, K. K. *J. Mol. Spectrosc.* **1986**, *120*, 1.
(30) Lim, E. C. *J. Phys. Chem.* **1986**, *90*, 6770.

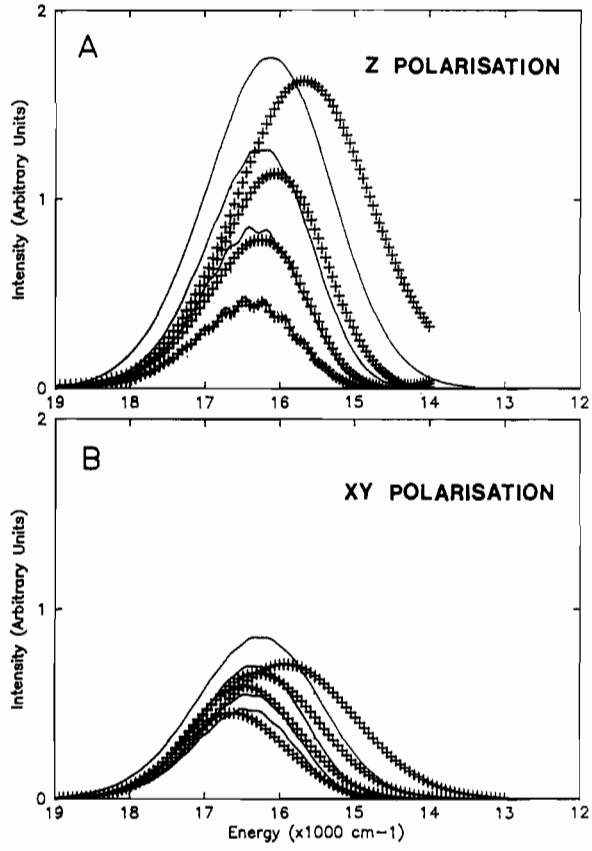


**Figure 6.** $^2A_{1g}(z^2) \leftarrow {}^2B_{1g}(x^2 - y^2)$ transition at, in order of increasing intensity, 10, 70, 140, and 265 K. Experimental points are shown as crosses and the full lines were calculated by using the excited-state potentials derived from the angular overlap model. The contributions to the intensity from the lower energy transitions have been subtracted from the experimental data; in the case of the spectrum in *xy* polarization the experimental points lie along the best-fit Gaussian curves to the experimental data.

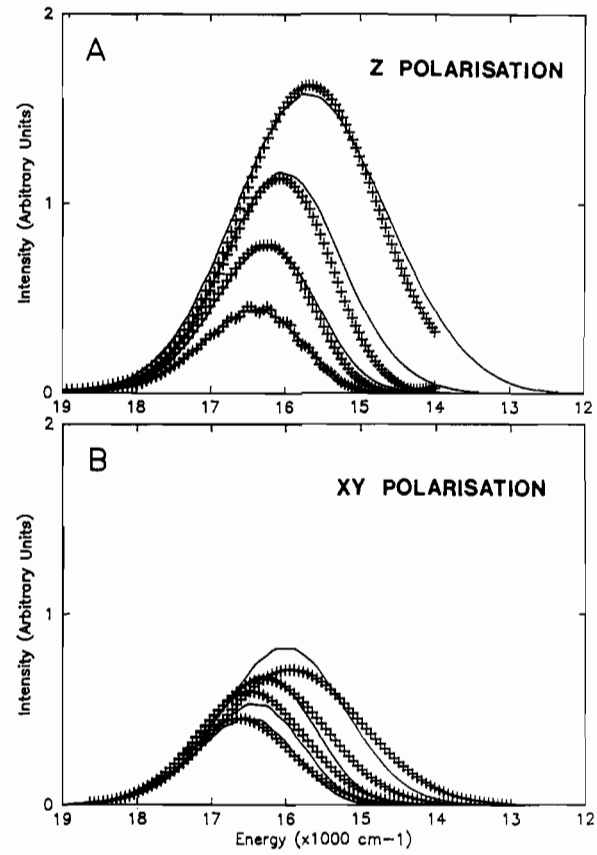


**Figure 7.** $^2A_{1g}(z^2) \leftarrow {}^2B_{1g}(x^2 - y^2)$ transition at, in order of increasing intensity, 10, 70, 140, and 265 K. Experimental points are shown as crosses and the full lines were calculated using the excited-state potentials derived using the angular overlap model except for that of the $\beta_{2u}$ potential, which is given by curve 1 of Figure 3. The contributions to the intensity from the lower energy transitions have been subtracted from the experimental data; in the case of the lowest energy spectrum in *xy* polarization the experimental points lie along the best-fit Gaussian curve to the experimental data.

respects, while for the *xy* spectrum the only feature that is reproduced poorly is the bandwidth at higher temperatures. However, this last discrepancy is not unexpected. The $\beta_{2u}$ mode is noninducing in *xy* polarization, and the fact that the excited-state surface differs dramatically from the ground state in this coordinate will cause the vibronic origins in the inducing $\epsilon_u$ vibration to develop a band structure similar to that discussed for the $\beta_{2u}$ mode in the following section. This structure will increase with the thermal population of higher levels of the $\beta_{2u}$ vibration in the ground state and will hence give rise to a width for the individual lines built on the $\epsilon_u$ origins that increases with temperature. With the introduction of such a temperature-dependent fundamental line width, the high-temperature spectra in *xy* polarization could be fitted virtually perfectly. It must also be remembered that a small fraction of the intensity in this polarization ($\sim$6% at low temperature) is due to coupling with a low energy ($h\nu \simeq 80$ sm$^{-1}$) lattice mode.[5] This has been included in the present calculations by an arbitrary 6% reduction in the "effective" energy of the $\epsilon_u$ vibration, and this approximation will also introduce inaccuracies in the calculated line shapes.

### Basic Cause of the $^2A_{1g}(z^2) \leftarrow {}^2B_{1g}(x^2 - y^2)$ Band Maximum Shift

Although the spectral line shape is caused predominantly by bands in the $\alpha_{1g}$ mode, the shifts in band maximum are due almost exclusively to changes in the vibronic origins, with either temperature or polarization. It is therefore instructive to look at the appearance of the spectrum in the absence of the $\alpha_{1g}$ band structure, and this is shown in Figure 8a for the transitions between the $\beta_{2u}$ levels in *z* polarization. Here, the "vibronic origin" is seen to increase in both intensity and half-width and to shift to lower energy as the temperature rises. The basic cause of this may be seen in the plot shown in Figure 8b, where the fundamental width of the individual lines has been made very small. It can be seen that the simple selection rules of vibronic coupling, which are based upon identical ground- and excited-state vibrational potentials, and where all the intensity of a parity-forbidden transition is built upon the change of a single quantum of the inducing mode, break down. At low temperature, the single peak that serves as a "vibronic origin" for the $\alpha_{1g}$ progression is seen to be composed of a band itself, formed by transitions from the zero level of the $\beta_{2u}$ mode in the ground state, to various levels of the double-minimum excited-state potential surface (Figure 3). As the temperature is increased, new bands arise due to excitations from the higher vibrational levels of the $\beta_{2u}$ mode in the ground state, leading to a very complicated basic pattern. However, the fundamental cause of the red shift of the overall band maximum is the fact that these higher levels will have greatly improved overlap with the lower vibrational levels in the excited-state minima.

The spectrum in *xy* polarization is expected to follow a basically similar pattern, except that here the "band structure" produced by the difference between the ground- and excited-state potential surfaces of the inducing $\epsilon_u$ mode will be far less pronounced. The basic cause of the large difference in the energy of the band maximum between *z* and *xy* polarization is the fact that in the former case, when the $\beta_{2u}$ mode is inducing, maximum overlap between the $\beta_{2u}$ potential surfaces occurs at a much lower energy than in the latter case. As already mentioned, a feature not included in the simulations is the fact that the large difference between the potential surfaces of the ground and excited states in the $\beta_{2u}$ coordinate will produce a "band structure" in the transitions between the $\epsilon_u$ levels, hence contributing to the basic line width of these transitions.

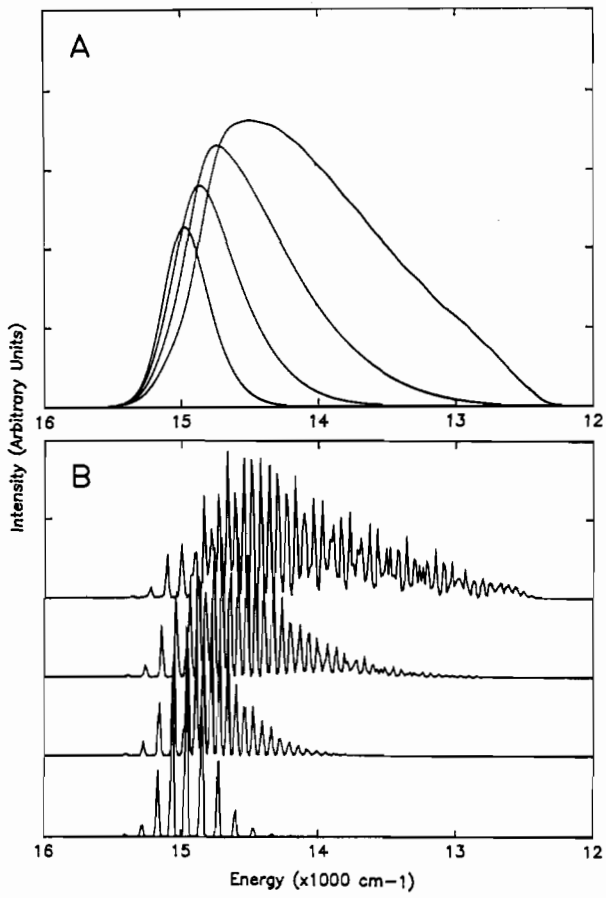


**Figure 8.** Calculated spectrum of the $^2A_{1g}(z^2) \leftarrow {}^2B_{1g}(x^2 - y^2)$ transition in $z$ polarization at, in order of increasing intensity, 10, 70, 140, and 265 K, ignoring the progressions in the $\alpha_{1g}$ totally symmetric stretching mode: spectrum A, low resolution (full width at half-height = 270 $cm^{-1}$); spectrum B, high resolution (full width at half-height = 25 $cm^{-1}$).

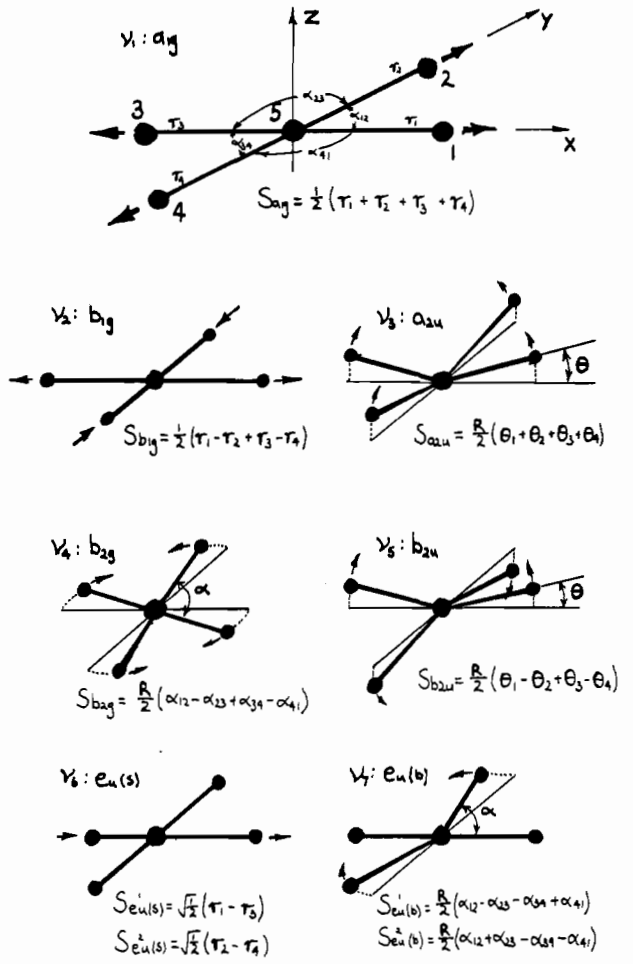


**Figure 9.** Molecular axes and symmetry coordinates of $CuCl_4^{2-}$. $R$ is the equilibrium bond length.

## General Conclusions and Suggestions for Future Work

From the temperature dependence of the intensity of the $^2A_{1g}(z^2) \leftarrow {}^2B_{1g}(x^2 - y^2)$ transition, it appears that the ground-state potential surface of the planar $CuCl_4^{2-}$ ion must be relatively unexceptional, except that the out-of-plane bending vibration of $\beta_{2u}$ symmetry is slightly anharmonic and of very low energy. This provides a useful constraint in considering the cause of the unusually large red shift of the band maximum on warming from 10 to 295 K. It would seem that this latter feature is quite incompatible with an excited-state potential surface which is similar to that in the ground state. It appears that good agreement between simulated spectra and those observed experimentally can be obtained only if the potential surface of the excited state is highly distorted in the $\beta_{2u}$ normal coordinate, with a double minimum corresponding to an equilibrium nuclear geometry that is not planar, but distorted toward two equivalent pseudotetrahedral ligand arrangements. The large red shifts observed for the other electronic transitions imply that a similar distortion occurs in these excited states also.

The very similar trends in the temperature dependence of the electronic spectra of all compounds containing planar $CuCl_4^{2-}$ ions suggest that a distortion in the excited electronic states of the above kind is a general feature of this complex. In considering why this particular species behaves in this anomalous manner (it must be remembered that, to first order, a distortion in nondegenerate excited states is allowed only in vibrations of $\alpha_1$ symmetry), it is probably relevant that the energy barrier to a displacement along the normal coordinate which transforms the complex from a planar toward a tetrahedral ligand geometry is apparently very small. This is indicated by the fact that with different counterions the trans ClCuCl angle varies widely, covering the range 180 to ~129°.[26] In fact, it has been suggested by Bacci[21] that in some four-coordinate copper(II) complexes with pseudotetrahedral geometries the vibrational mode in question may not only be of very low energy but be highly anharmonic, so that the average root-mean-square angular displacement from planarity will be temperature dependent. It was proposed that dynamic behavior of this kind may be important in biologically active copper(II) complexes, by providing low-energy reaction pathways (it is noteworthy that the spectral properties of $CuCl_4^{2-}$ have been proposed as a useful model of the "blue" copper(II) proteins[28,31]). It would be of interest to study the temperature dependence of the electronic spectra of compounds containing pseudotetrahedral ions, including those involving $CuCl_4^{2-}$, to see whether these exhibit band shifts similar to those discussed by Bacci.[21] However, for these systems it might be hard to distinguish between a distorted geometry in the excited state, and an anharmonic ground-state potential surface, since variations in band intensity would give little information, as the transitions are parity allowed.

The present model suggests that the fine structure observed at low temperature in the spectra of compounds containing planar $CuCl_4^{2-}$ is probably due to the superposition of many vibronic lines. The position of these fundamental components is expected to be quite sensitive to the shape of the distorted excited-state potential surface, which in turn is likely to be strongly influenced by the crystal lattice (it must be remembered that it is lattice forces such as hydrogen bonding that are thought to stabilize the planar geometry of the complex in the ground state). It has been noticed that although the geometries of the planar $CuCl_4^{2-}$ ions in the three compounds currently known to contain this complex are virtually identical, the extent to which vibrational fine structure is resolved in their low-temperature optical spectra differs dramatically, and it has been generally assumed that variations in

(31) Solomon, E. I.; Penfield, K. W.; Wilcox, D. E. *Struct. Bonding (Berlin)* **1983**, *53*, 1.

**Table II.** Point Groups of the $CuCl_4^{2-}$ Ions Distorted along Different Symmetry Coordinates

| vibration | instantaneous point groups | irreducible representations | | | | |
|---|---|---|---|---|---|---|
| | | $d_{z^2}$ | $d_{x^2-y^2}$ | $d_{xy}$ | $d_{xz}$ | $d_{yz}$ |
| $\nu 3$ ($\alpha_{2u}$) | $C_{4v}$ | $A_1$ | $B_1$ | $B_2$ | E | |
| $\nu_4$ ($\beta_{2g}$) | $D_{2h}$[a] | $A_g$ | $B_{1g}$ | $A_g$ | $B_{2g}$, $B_{3g}$ | |
| $\nu 5$ ($\beta_{2u}$) | $D_{2d}$[a] | $A_1$ | $B_2$ | $B_1$ | E | |
| $\nu 7$ ($\epsilon_u$(b)) | $C_{2v}$ | $A_1$ | $A_1$ | $B_1$ | $B_2$ | $A_2$ |

[a] A "nonstandard" point group; the molecular axes are as defined in Figure 9.

**Table III.** Angular Overlap Matrix Elements for $CuCl_4^{2-}$ Ions Distorted along Different Symmetry Coordinates[a]

$\alpha_{2u}$ and $\beta_{2u}$ Type Distortions

$\langle z^2|V|z^2\rangle = {}^1/_4(1 - 3\cos 2\theta)^2 e_\sigma + (3\sin^2 2\theta)e_\pi - 16(\sin^2\theta - {}^1/_2\cos^2\theta)^2 e_{ds}$
$\langle x^2 - y^2|V|x^2 - y^2\rangle = 0.75(1 + \cos 2\theta)^2 e_\sigma + (\sin^2 2\theta)e_\pi$
$\langle xy|V|xy\rangle = 4(\cos^2\theta)e_\pi$
$\langle xz|V|xz\rangle = 1.5(\sin^2 2\theta)e_\sigma + 2(\sin^2\theta + \cos^2 2\theta)e_\pi$
$\langle yz|V|yz\rangle = 1.5(\sin^2 2\theta)e_\sigma + 2(\sin^2\theta + \cos^2 2\theta)e_\pi$

$\beta_{2g}$ Type Distortion

$\langle z^2|V|z^2\rangle = e_\sigma - 4e_{ds}$
$\langle x^2 - y^2|V|x^2 - y^2\rangle = 3(\sin^2\alpha)e_\sigma + 4(\cos^2\alpha)e_\pi$
$\langle xy|V|xy\rangle = 3(\cos^2\alpha)e_\sigma + 4(\sin^2\alpha)e_\pi - 48(\cos^2\alpha)e_{ds}$
$\langle xz|V|xz\rangle = 2e_\pi$
$\langle yz|V|yz\rangle = 2e_\pi$
$\langle xz|V|yz\rangle = \langle yz|V|xz\rangle = 2(\cos\alpha)e_\pi$
$\langle z^2|V|xy\rangle = \langle xy|V|z^2\rangle = -3^{1/2}(\cos\alpha)e_\sigma$

$\epsilon_u$(b) Type Distortion

$\langle z^2|V|z^2\rangle = e_\sigma - 4e_{ds}$
$\langle x^2 - y^2|V|x^2 - y^2\rangle = {}^3/_2(1 + \cos^2 2\alpha)\, e_\sigma + 2(\sin^2 2\alpha)e_\pi - 48(\cos^4\alpha)e_{ds}$
$\langle xy|V|xy\rangle = {}^3/_2(\sin^2 2\alpha)e_\sigma + 2(1 + \cos^2 2\alpha)e_\pi$
$\langle xz|V|xz\rangle = 2(1 + \cos^2\alpha)e_\pi$
$\langle yz|V|yz\rangle = 2(\sin^2\alpha)e_\pi$
$\langle z^2|V|x^2 - y^2\rangle = \langle x^2 - y^2|V|z^2\rangle = -3^{1/2}/2(1 + \cos 2\alpha)e_\sigma$

[a] Note: The internal coordinates $\theta$ and $\alpha$ are defined in Figure 9.

**Table IV.** Coefficients Defining the Change in Energy of the Excited d States with Respect to the Symmetry Coordinates[a]

| vibration | $\nu_3$ | $\nu_4$ | $\nu_5$ | $\nu_7$ |
|---|---|---|---|---|
| symmetry | $\alpha_{2u}$ | $\beta_{2g}$ | $\beta_{2u}$ | $\epsilon_u$(b) |
| frequency, $cm^{-1}$ | 159 | 181 | 60 | 165 |
| $a_2$ | 0.5 | 0.5 | 0.5 | 0.5 |
| $c_2$, $cm^{-1}$ $deg^{-2}$ | 25.37 | 26.55 | 11.67 | 20.86 |
| → $d_{z^2}$ transition | | | | |
| $c_2$, $cm^{-1}$ $deg^{-2}$ | −13.148 | 2.020 | −13.148 | −7.408 |
| $c_4$, $cm^{-1}$ $deg^{-4}$ | 0.00392 | 0.01864 | 0.00392 | −0.00258 |
| $a_2$ | −0.2592 | 0.0380 | −0.5632 | −0.1776 |
| $a_4$ | 0.00024 | 0.00120 | 0.00043 | −0.00055[c] |
| → $d_{xz}$ transition[b] | | | | |
| $c_1$, $cm^{-1}$ $deg^{-1}$ | 0.0 | 31.416 | 0.0 | 0.0 |
| $c_2$, $cm^{-1}$ $deg^{-2}$ | −16.435 | −3.701 | −16.435 | −6.859 (−7.956) |
| $c_3$, $cm^{-1}$ $deg^{-3}$ | 0.0 | −0.00159 | 0.0 | 0.0 |
| $c_4$, $cm^{-1}$ $deg^{-4}$ | 0.00484 | 0.00037 | 0.00484 | −0.00312 (−0.003) |
| $a_1$ | 0.0 | 0.3204 | 0.0 | 0.0 |
| $a_2$ | −0.324 | −0.069 | −0.704 | −0.164 (−0.191) |
| $a_3$ | 0.0 | −0.00006 | 0.0 | 0.0 |
| $a_4$ | 0.00030 | 0.00002 | 0.0053 | −0.00030 (−0.00029) |
| → $d_{xy}$ transition | | | | |
| $c_2$, $cm^{-1}$ $deg^{-2}$ | −7.397 | 8.809 | −7.397 | −14.807 |
| $c_4$, $cm^{-1}$ $deg^{-4}$ | 0.00181 | −0.0197 | 0.00181 | −0.00013 |
| $a_2$ | −0.1458 | 0.1659 | −0.3169 | −0.3549 |
| $a_4$ | 0.00011 | −0.00127 | 0.00020 | −0.00001 |

[a] Only nonzero coefficients are given. A least-squares polynomial of degree 4 is fitted to 31 points in the range ±15°. [b] For the → $d_{yz}$ transition change the sign of $c_1$ and $c_3$ and use the parenthetical quantities for $c_2$ and $c_4$. [c] This small negative quartic term would cause the potential to become unbound for a large distortion of the $e_g$ coordinate. In the variational calculations this was therefore set equal to zero.

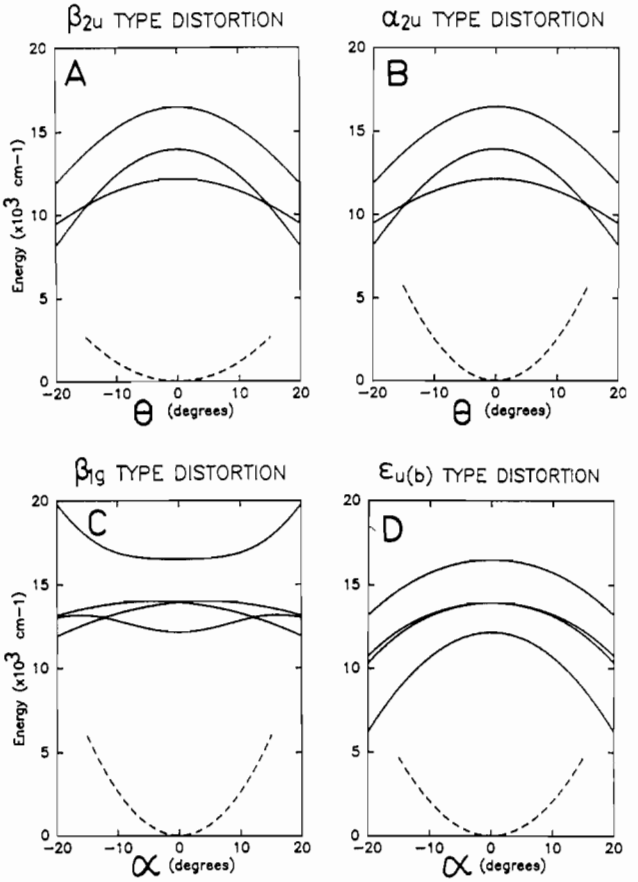


**Figure 10.** Energies of the excited d states relative to the ground state for distortions along the (A) $\beta_{2u}$, (B) $\alpha_{2u}$, (C) $\beta_{1g}$, or (D) $\epsilon_u$ symmetry coordinates. Ground-state vibrational potentials are also shown. The coordinates $\theta$ and $\alpha$ are defined in Figure 9.

the coupling between the lattice and ground-state metal–ligand vibrational modes are probably responsible for this difference.[4,5] The present study suggests that differences in the *excited*-state potential surfaces of the complexes may perhaps also be important. Moreover, the previous interpretations of the vibrational fine structure, which have involved the consideration of metal–ligand vibrations within the framework of simple vibronic coupling theory, supplemented by coupling with lattice modes, may also need to be reconsidered in the light of the present conclusions.

**Acknowledgment.** We thank R. G. McDonald for many useful discussions and for making available experimental data and the Australian Research Grants Scheme for financial assistance.

## Appendix A. Analytic Formulas in the Harmonic Approximation

The derivation of the "coth" rules given in (13) and (14) has been reported by several workers.[2a,11] Similarly, the expressions for the mean energy and half-width of an electronic transition due to noninducing modes in (15) and (16) have been reported previously.[11,13] Here, the analogous expressions for inducing modes are derived.

Assuming a linear dependence of the electronic transition moment on an inducing coordinate, from (11) the mean energy of a transition is

$$E(T) = \sum_{ij}(\epsilon_j - \epsilon_i)/\sum_{ij} \qquad \text{(A1)}$$

where $\sum_{ij}$ is shorthand for $\sum_i P_i(T)\sum_j|\langle i|\xi|j\rangle|^2$. If it is assumed that the potential surfaces are harmonic and identical in the ground and excited states, the overlap $\langle i|\xi|j\rangle$ is nonzero only when $j = i \pm 1$. Relative to the electronic origin, the mean energy of the transition is

$$E(T) = \sum_i P_i(T)[h\nu(i+1) - ih\nu]/(1+X)/(1-X)$$
$$= h\nu\sum_i X^i(1-X)^2/(1+X)$$
$$= h\nu \tanh Y \qquad \text{(A2)}$$

Here $X = \exp(-h\nu/kT)$, $Y = h\nu/2kT$, and $h\nu$ is the frequency of the inducing vibration.

The expression for the half-width, again assuming identical harmonic potentials in the ground and excited states, from (12) is

$$H(T) = 2(2(\ln 2)\Lambda_2)^{1/2} \qquad \text{(A3)}$$

where

$$\Lambda_2 = \sum_{ij}(\epsilon_j - \epsilon_i - E(T))^2/\sum_{ij}$$

$$=(h\nu)^2\sum_i P_i(T)[i(1+\tanh Y)^2 + (i+1)\times (1-\tanh Y)^2]/(1+X)/(1-X)$$

$$=(h\nu \text{ sech } Y)^2(1-X)^2\sum_i X^i(iX^{i-1} + (i+1)X^{i+1})/(1+X)/(1-X)$$

$$=(h\nu \text{ sech } Y)^2$$

This then gives

$$H(T) = 2(2(\ln 2))^{1/2}h\nu \text{ sech } Y \qquad \text{(A4)}$$

## Appendix B. Estimation of Excited-State Potential Surfaces with the Angular Overlap Model

Adiabatic potential surfaces may be found by solving an electronic Hamiltonian at fixed nuclear geometries of the molecule. Here, the energies of the ligand field electronic states are calculated relative to the ground state along the symmetry coordinates of the complex, and for the particular excited d state of interest, this is added to the vibrational potential of the ground state to yield the required potential surface. It should be noted that this approach neglects the influence of charge-transfer states on the form of the potential surface. These may well be important in the present case, since it is coupling with these states along the inducing symmetry coordinates that provides the observed intensity of the transitions. It is known that the effect of vibronic coupling can often be to produce a lower potential surface with a double minimum, such as that proposed for the present complex, this often being referred to as a pseudo-Jahn–Teller effect.[32]

The molecular coordinate system and symmetry coordinates of planar $CuCl_4^{2-}$ are shown in Figure 9. In the following treatment, only bending vibrations are considered, as these are of lower energy than the stretching vibrations[5] and therefore should be more important in the present problem. Moreover, simple arguments show that the potential surfaces of the stretching vibrations cannot be responsible for the observed anomalous band shifts. The $\alpha_{1g}$ mode cannot make a significant contribution, as its excited-state potential is known to be harmonic from the progressions seen in the electronic spectra. The remaining stretching modes, $\beta_{1g}$ and $\epsilon_u(s)$, both involve the approach of two ligands, while the other two move away (Figure 9), which will have little effect on the d-orbital energies.

The angular overlap model (AOM) provides a convenient way to calculate the required potentials (though it should be noted that the expressions to be used depend only on the angular relationships between the ligands and the d orbitals and bonding parameters derived from the electronic spectrum of the planar complex and are hence independent of the extent to which the bonding is ionic or covalent). The instantaneous point groups of a complex "frozen" along each of the relevant symmetry coordinates are given in Table II. These determine which d-orbital basis functions will be mixed by the ligand field. The ligand field matrix elements are given in Table III. Note that those for distortions along the $\beta_{2u}$ and $\alpha_{2u}$ coordinates are identical. Smith[33] has pointed out that the totally symmetric basis functions may mix with the metal 4s orbital, and this is taken into account by using extra group overlap integrals and a bonding parameter $e_{ds}$.[33,34]

With the expressions in eq A2, and the bonding parameters $e_\sigma = 5250\ cm^{-1}$, $e_\pi = 900\ cm^{-1}$, and $e_{ds} = 1500\ cm^{-1}$, which reproduce the observed transition energies of planar $CuCl_4^{2-}$,[5] the variation of the excited-state energies as a function of the four bending coordinates were calculated, and the results are shown in the Figure 10a–d. The appropriately dimensioned ground-state potential is also included for comparison. These curves were fitted to a fourth-order polynomial by a least-squares procedure, and the results are presented in Table IV.

Care must be taken when converting from the internal coordinates ($\theta$, $\alpha$) to symmetry coordinates ($S$ in Figure 9) and dimensionless coordinates ($\xi$), and to avoid confusion this is outlined in detail for the $\beta_{2u}$ mode. In all the plots of the potential surfaces, the internal coordinates have been used. For the $\beta_{2u}$ mode this corresponds to the four equal displacements in $\theta$ along the directions indicated by the symmetry coordinate in Figure 9. That is, $\theta = 0°$ and $\theta = 35.26°$ correspond to planar and tetrahedral geometries, respectively. The potentials can be defined as

$$V(\beta_{2u}) = c_0 + c_1\theta + c_2\theta^2 + \ldots \qquad \text{(A5)}$$

$$V(\xi) = a_0 + a_1\xi + a_2\xi^2 + \ldots \qquad \text{(A6)}$$

where the coefficients $c_i$ have the dimensions ($cm^{-1}$ $deg^{-i}$) and the coefficients $a_i$ are dimensionless. These coefficients are related by

$$h\nu a_i = (180/(2\pi Rx))^i c_i \qquad \text{(A7)}$$

The coordinates are related by

$$\theta = (180/(2\pi Rx))\xi \qquad \text{(A8)}$$

Here $R$ is the equilibrium bond length in picometers and $x$ is a constant previously given in (18).

For the other bending modes identical equations are obtained after the appropriate substitutions are made ($\alpha \rightarrow \theta$, for example), *except* for the mass $M$ used in the constant $x$. This is the inverse of the appropriate element of the G matrix[15] and will differ for each mode:

$$\beta_{2u}:\ M = m(Cl)$$
$$\alpha_{2u}:\ M = m(Cl)M(Cu)/[4m(Cl) + m(Cu)]$$
$$\beta_{2g}:\ M = m(Cl)/4$$
$$\epsilon_u(b):\ M = m(Cl)m(Cu)/[4m(Cl) + 2m(Cu)] \qquad \text{(A9)}$$

The $\epsilon_u(b)$ mode is complicated by the fact that it is coupled to the stretching mode of the same symmetry; here it is assumed that such coupling is negligible.

**Discussion.** As required by group theory (Table II) the degeneracy of the $d_{xz}$ and $d_{yz}$ orbitals is removed by distortions along the $\beta_{2g}$ and $\epsilon_u(b)$ symmetry coordinates. This is caused by linear and quadratic terms in the potentials, corresponding to a Jahn–Teller effect and a Renner–Teller effect, respectively.

When the electronic potentials are added to the ground-state vibrational potentials, the effect is generally to create a near-harmonic excited state with a decreased force constant. The exception is the $\beta_{2u}$ mode, where the low energy of the ground-state potential is such that a double-minimum excited-state potential results, as shown in Figure 3. As discussed in the text, this potential is probably only qualitatively correct, and it seems likely that vibronic coupling with charge-transfer states acts to reinforce the double minimum of the potential.

**Registry No.** $CuCl_4^{2-}$, 15489-36-8.

(32) Gustav, K.; Cojditz, R. *J. Quant. Chem.* **1983**, *24*, 327.

(33) Smith, D. W. *Inorg. Chim. Acta* **1977**, *22*, 107.

(34) Kettle, S. F. A. *Inorg. Chem.* **1965**, *4*, 1821.